Science of the Total Environment 659 (2019) 1293–1306

Contents lists available at ScienceDirect

Science of the Total Environment

journal homepage: www.elsevier.com/locate/scitotenv

Water resources and nitrate discharges in relation to agricultural land uses in an intensively irrigated watershed

R. Sorando [a,b,*], F.A. Comín [a], J.J. Jiménez [c], J.M. Sánchez-Pérez [d], S. Sauvage [d]

[a] Instituto Pirenaico de Ecología-CSIC, Av. Montañana 1005, 50192 Zaragoza, Spain
[b] AISECO, C/Enrique Val 41, 3°. 50011 Zaragoza, Spain
[c] Instituto Pirenaico de Ecología-CSIC, Av. Ntra. Sra. de la Victoria 16, 22700 Jaca, Huesca, Spain
[d] ECOLAB, UMR 5245 CNRS/UPS/INPT, ENSAT, Av. Agrobiopole BP32607 Auzeville Tolosane, 31326 Castanet Tolosan, France.

HIGHLIGHTS

- Modeling water resources and nitrate pollution in an agricultural catchment
- Green water storage and green water flow are the dominant of the water balance
- Nitrate infiltration in the aquifer is higher in the irrigated subwatersheds
- Lateral flow is higher in the non-irrigated subwatersheds
- High potential to improve the benefits of water cycles in agricultural watersheds

GRAPHICAL ABSTRACT

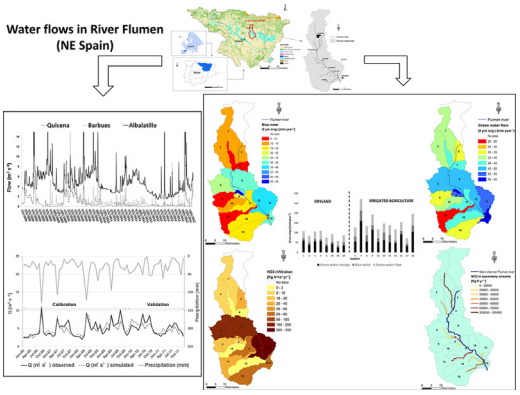

ARTICLE INFO

Article history:
Received 14 August 2018
Received in revised form 3 December 2018
Accepted 3 December 2018
Available online 13 December 2018

Editor: Ouyang Wei

Keywords:
Water resources
Nitrate
SWAT model
Calibration
Validation
Sensitivity analysis

ABSTRACT

Application of integrated hydrological models to manage water resources and non-point agricultural pollutants are increasingly used in decision-making processes. In this study SWAT (Soil and Water Assessment Tool) was used to simulate the water balance and nitrate pollution in an intensively irrigated agricultural catchment (Flumen River in Monegros, Aragon, NE Spain). Rainfall comprised only 45% of the inputs of water in the Flumen watershed and the rest is contributed through irrigation canals from two other rivers outside the Flumen watershed. Green water storage and green water flow are the dominant components of the water balance in the watershed, which is related to the important contribution of water for irrigation. In general, green water storage and green water flow are quite similar in the subwatersheds dominated by irrigation agriculture that are located in the central part of the watershed. A similar pattern was observed for blue water, with high amounts in the central irrigated subwatersheds compared to the non-irrigated subwatersheds. Consequently, nitrate infiltration in the aquifer was higher in the inner irrigated subwatersheds (100–250 kg N ha^{-1} $year^{-1}$) but much lower than the lateral flow rates estimated in the non-irrigated subwatersheds (1400–2000 kg N ha^{-1} $year^{-1}$). Two scenarios simulating the effects of expected climate change factors in this zone were performed. A reduction in the availability of water for irrigation will transform the area from irrigated crops to cereal. In this case the water flow of River Flumen at the outlet of the watershed is reduced by 15%. If a reduction of 40% nitrate fertilization is applied, the nitrate

* Corresponding author at: Instituto Pirenaico de Ecología-CSIC, Av. Montañana 1005, 50192 Zaragoza, Spain and AISECO, C/Enrique Val 41, 3°. 50011 Zaragoza, Spain.
E-mail address: ricsorando@ipe.csic.es (R. Sorando).

https://doi.org/10.1016/j.scitotenv.2018.12.023
0048-9697/© 2018 Elsevier B.V. All rights reserved.

exported to Flumen River would decreased by 28%. These results suggest that dosing irrigation water and fertilizers in accordance with crop requirements would contribute to buffer peaks of water and nitrate discharges and to a more efficient agricultural use of the resources.

© 2018 Elsevier B.V. All rights reserved.

1. Introduction

In agricultural zones with intensive irrigation and use of fertilizers, surface water and groundwater are subjected to pollution (Tilman et al., 2002). Nitrate discharges from agricultural uses and pollution of aquifers and rivers is common worldwide (Ullrich and Volk, 2009). Hence, regulations such as the European Water Framework Directive (WFD) aim to achieve a good ecological status for water bodies. However, due to the diffuse nature of this type of pollution, emissions cannot be imputed with precision, neither in space nor in time. This makes it difficult to evaluate current or planned measures to reduce these emissions. Eco-hydrological simulation models allow a precise understanding and simulation of nitrate pollution processes resulting from agricultural activity. Moreover, this type of analysis can be validated by comparison with field measurements. Usually, these models require a large amount of data and expertise. Indicators have therefore been developed to tackle these difficulties and to introduce decision support tools (Lacroix et al., 2006). Simulation models, like SWAT, are essential tools for decision support in water resources planning, since it was designed to be applied to catchment areas ranging from a few hundred to several thousand square kilometers (Arnold et al., 1998).

The dynamics of nitrogen (N) in agricultural watersheds has been studied at different spatial scales and at different sampling frequencies (Ferrant et al., 2013). A substantial portion of the N used as fertilizer is exported from land to aquatic ecosystems (Seitzinger and Harrison, 2008). SWAT simulates nitrate losses as runoff, percolation and lateral surface flow. The model includes nitrogen transformations and residue mineralization, nitrification, denitrification, volatilization, fertilization and plant uptake (Srinivasan et al., 1998). Under similar agricultural conditions, the export of N increases with the percentage of agricultural area in the watershed (Kaushal et al., 2008). In zones with irrigated agriculture, irrigation return flows (IRF) are a key factor regulating the concentration of nitrate in surface waters (Causapé et al., 2006). IRF also have the potential for disrupting the natural hydrologic water balance of river basins (Haddeland et al., 2006). However, weather conditions also influence nitrate mobilization (Darwiche-Criado et al., 2015a, 2015b). Thus, it is very useful to ascertain the drivers of water and nitrate flows in the rivers draining watersheds and relate them with respect to spatial and temporal land uses (Oeurng et al., 2011a, 2011b).

The objectives of this paper are i) to model the spatial-temporal variations of water and nitrate discharges in an intensively irrigated agricultural watershed, the Flumen River watershed in North Monegros (NE Spain); ii) to estimate the major components of the water balance, such as blue water (considered as water yield plus deep aquifer recharge), green water flow (evapotranspiration) and green water storage (soil moisture); and iii) to identify major non-point sources of pollution in this watershed. This paper approaches modeling water and nutrient balances and intensively mediated water and nutrient flows by human uses which, in spite of adding uncertainty to the modeling process, results in useful information for land and natural resources management (Gassman et al., 2014), particularly in watersheds with extensively irrigated agricultural lands.

2. Study area

The Flumen River watershed (1271 km^2) is located in the Ebro River Basin (NE Spain) (Fig. 1A).

It has only one permanent tributary, the Isuela River. The northern part of the watershed is a medium mountain zone made of conglomerates and calcareous rocks. The central and southern parts of the watershed are plains that are mostly used for intensive irrigated agricultural practices, with clay and silty soils and some gravel materials near the river channels. The margins of this watershed are non-irrigated areas, mostly used for dry agriculture, and the major types of soils are gypsisols, leptosols and calcisols. The margins of the watershed are low altitude mountain ranges occupied by forests and pastures (Fig. 1E).

Most of the watershed is quite flat, with slopes lower than 5%. Altitudes range from 230 m.a.s.l. in the southernmost zone of the basin to 1694 m.a.s.l. in the northern part where a mountain range is located. Correspondingly, climate conditions range from semi-humid in the northern part to semi-arid in the central and southern parts. The annual average rainfall in the study area (413 mm year^{-1}) is not representative because there is a high interannual variability of 32.7% (Comín and Williams, 1994) and because heavy storms take place during the summer months. The average annual temperature is 14.5 °C in the central part of the basin. The highest average temperature is observed in July (26 °C) and the lowest in January (5 °C). Evapotranspiration is high (800–1000 mm year^{-1}).

Two canals with water from the Cinca and Gállego Rivers cross, respectively, northeast and northwest of the Flumen Watershed and flow parallel to the Flumen River through watersheds located, respectively, at the east and west of the River Flumen watershed. These two rivers originate in the Pyrenees Mountains. Water is thus distributed through a dense network of constructed, cemented or piped canals all around the irrigated central and southern areas of the Flumen Watershed (Fig. 1D). The irrigated agricultural zone mostly used for maize (*Zea mays*), alfalfa (*Medicago sativa*), barley (*Hordeum vulgare*) and rice (*Oryza sativa*) production is part of the largest irrigation system in Europe (Riegos del Alto Aragón) and is drained by a dense network of channels excavated in the soil to drain the excess irrigation water towards the Flumen River, which also transports suspended solids and dissolved compounds exported from the agricultural fields. In some zones, soil salinity often results from the salt that is concentrated at the surface by evapotranspiration. Puddled rice is a sound productive choice for agriculture in saline inland areas where irrigation water with low electrical conductivity is available. This commodity has been grown for approximately 60 years as the only economically feasible crop due to soil salinity. As long as the soil is flooded, the irrigation water prevents the saline groundwater underneath the puddle zone from contaminating the paddy rice rooting zone. The oldest and most typical paddy rice fields in Flumen are located in landscape depressions (Herrero and Hudnall, 2014).

Some parts of the Flumen River watershed are located at higher altitudes than the canals transporting water for irrigation of the central irrigated zone. These areas, which are mostly located at the margins of the watershed, are used for dry agriculture (mostly barley and wheat) but also include natural forest, reforested Pinus woods and pasture lands.

The water discharge of River Flumen, which is recorded at the gauging stations (Figs. 2 and 3) represents very well the dominant land uses in each sector of the watershed. The flow of the River at Quicena represents the forested area of the watershed, with little human intervention. In Barbues, the river has already seeped into the northernmost irrigation zone and has received the contribution of its main tributary, that runs through Huesca (53,000 inhabitants), the most important city of the watershed. There is still no increase in flow. It is at the outlet, in Albalatillo, where all the IRF is collected and where there is already a considerable increase of flow and, in addition, an alteration of the natural seasonality of the flow, with peaks in the summer months, i.e., when agricultural activity is more intense.

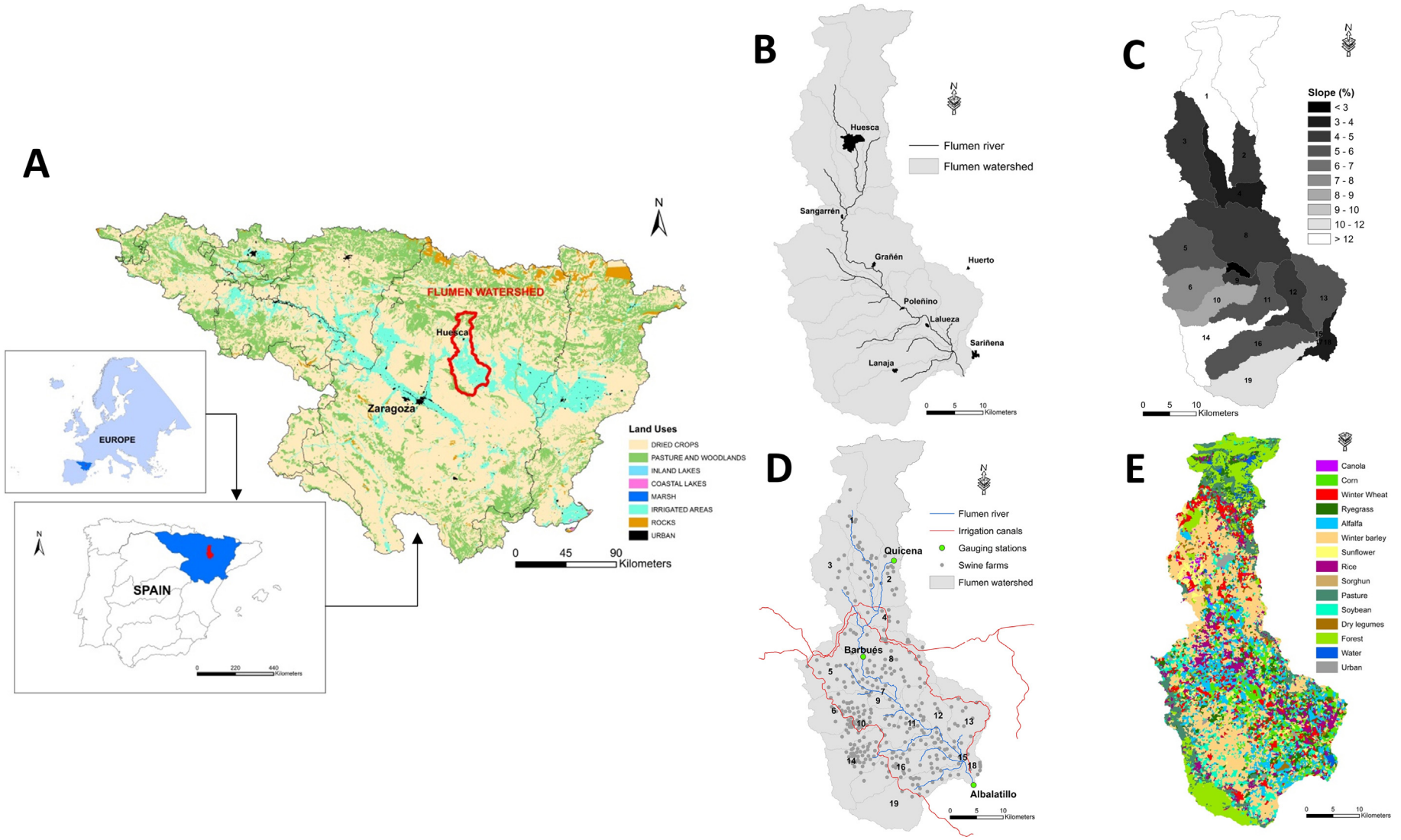

Fig. 1. A. Location of the Flumen River watershed in the Ebro River Basin. B. River Flumen watershed, its affluent Isuela River, which runs through the city of Huesca, and major temporary streams with their respective subwatersheds delimited by SWAT. C. Average slope of each subwatershed of the Flumen River watershed. D. Flumen River watershed showing the network of irrigation canals, the location of gauging stations in Flumen River, and the numbers of the subwatersheds simulated. Subbasins 5, 7, 8, 9, 11, 12, 13, 15, 16, 17 and 18, are located mostly in the intensive agricultural area. E. Distribution of major land covers in the River Flumen watershed (Right).

3. Materials and methods

We used the free software ArcSWAT 2012 and SWAT-CUP 5.1.6.2 to model the water and nitrate (NO_3^-) flows in the Flumen watershed combined with ArcGIS (versión 10.1). Using SWAT and a 40 m × 40 m digital elevation model (DEM), the River Flumen basin was subdivided in 19 subwatershed, and 432 Hydrologic Response Units (HRUs). These are areas with similar slope, soil and land use characteristics. The SWAT model can be divided as follows: hydrology, weather, sedimentation, soil temperature, crop growth, nutrients, pesticides and agricultural management. The simulated hydrologic processes include surface runoff, estimated from daily rainfall using the SCS curve number; percolation, modeled with a layered storage routing technique combined with a crack flow model; lateral subsurface flow; groundwater flow to streams from shallow aquifers; potential evapotranspiration, estimated by the Hargreaves, Priestley-Taylor and Penman-Monteith methods (Moriasi et al., 2007); transmission losses from streams; and water storage and losses from ponds.

Basic information used with SWAT were recent maps (DEM, land use and type of soil) obtained from air photographs ("Plan Nacional de Ortofotografía Aérea. Instituto Geográfico Nacional" -flight PNOA, 2009-). Data from the database of "Confederación Hidrográfica Ebro" (http://www.chebro.es) on the river water discharge at the gauging stations in Quicena, Barbues and Albalatillo were used (Fig. 1D). Additionally, meteorological data from official stations in Grañén, Huerto, Huesca, Lanaja and Sariñena were used (Fig. 1B).

We used SUFI-2 (Sequential Uncertainty Fitting version 2) of SWAT-CUP to calibrate and validate the model. Previous works showed that SUFI-2 is an efficient program to calibrate and quantify the uncertainty of hydro-ecological parameters of large (Faramarzi et al., 2009) and small watersheds (Abbaspour et al., 2007a, 2007b; Rostamian et al., 2008). Detailed information about the statistics used to calibrate and validate this model is given by Moriasi et al. (2007).

The Nash-Sutcliffe (NS) and coefficient of determination (R^2) statistics were used to calibrate the model. Additionally, the ratio standard deviation (RSR) and percent bias (PBIAS) were considered. NS ranges from $-\infty$ to 1. An efficiency of 1 ($E = 1$) corresponds to a perfect match of modeled and observed data. An efficiency of 0 ($E = 0$) indicates that the model predictions are as accurate as the mean of the observed data, whereas an efficiency less than zero ($E < 0$) occurs when the observed mean is a better predictor than the model. Essentially, the closer the model efficiency is to 1, the more accurate the model is.

The land use map (Fig. 1D) was elaborated from 5 satellite images (years 2002, 2005, 2006, 2007 and 2009) and corrected with land use data obtained from the regional Common Agricultural Policy databases of the years 2008 and 2009. The map of soil typologies used is that elaborated by the European Soil Data Center (http://eusoils.jrc.ec.europa.eu scale 1:1.000.000).

The water quality of the Flumen River at the watershed outflow (Albalatillo gauging station, Fig. 1D) was monitored continuously by an electronic device with a multiparametric sensor (YSI 6820) that recorded the water level and nitrates dissolved in the water every 10 min (Darwiche-Criado et al., 2015a, 2015b). It was connected to an automatic sampler collecting water in separate flasks every time there was a change of 30 cm in the water level (Supplementary material Observed data outlet gauging). Water samples were also collected by hand at this point weekly from October 2009–May 2011, preserved at low temperature (4 °C), and filtered and analyzed in the Instituto Pirenaico de Ecología (CSIC) laboratory for nitrate determination by ionic chromatography not later than one week after collection (Darwiche-Criado et al., 2015a, 2015b). Water samples were monthly hand collected at the outlet of all the subwatersheds of the study area with the same methodology used for the calibration of the Flumen basin model. Daily water flows were estimated after the calibration algorithm relating water level and discharge, as obtained from the water authority recording system (http://www.saihebro.com/saihebro/index.php?url=/datos/ficha/estacion:A094). Water flow was calculated from the rating curve, which is an indirect calculation. It is based on measuring in a known section of the river (m^2) the water velocity ($m\ s^{-1}$). Thus, multiplying section (m^2) by speed ($m\ s^{-1}$), it is estimated the water volume per unit of time ($m^3\ s^{-1}$). Technicians usually estimate a 10% of standard deviation (S.D.), although the most commonly used does not exceed 5% S.D. (https://www.iagua.es/blogs/conoce-che-y-gestion-agua/medicion-caudales-como-cuando-y-donde). Water infiltration and nitrate leached to the aquifer had not been taken into account because no data were available. It is presumably much lower than the subsurface flow since the entire irrigation area is drained by a dense network of pipes or drains.

Basic information about agricultural practices, fertilizer doses applied and other land uses (Table 1) was obtained from agrarian databases ("Anuario Estadístico Agrario de Aragón" 2012, http://www.aragon.es/DesarrolloRuralSostenibilidad/EstadisticasAgrarias) and from a survey of 35 farmers randomly distributed in the study area, as well as technicians in agrarian cooperatives.

Simulations of water and nitrate dynamics in the Flumen watershed were performed after running the SWAT model, SWAT-CUP calibration, model evaluation, a sensitivity analysis and SWAT-CUP validation, according to Arnold et al. (2012). The initial parameters and calibration ranges were selected according to our experience and the watershed characteristics, which are highly influenced by the network of drainage ditches in the irrigated area and the spatial and temporal distribution of the agricultural practices. Because nitrate discharge depends on water flows, the first step was calibrating the water balance and then nitrate discharges (Pohlert et al., 2005).

The period of simulation for water discharge was 2004–2011. The first two years were used to adjust the system and avoid previous conditions. Then, the calibration period was 2006–2009, and the validation period was 2010–2011. With respect to nitrate, the simulation period was only two years because of data availability. The calibration period was November 2009 to December 2010, and the validation period was the first half of 2011.

Simulation of water and nitrate flows with SWAT-CUP was performed at monthly and daily scales. In SUFI-2, the uncertainty in parameters, expressed as ranges (uniform distributions), accounts for all sources of uncertainty, such as uncertainty in driving variables (e.g., rainfall), the conceptual model, parameters, and measured data. Propagation of the uncertainties in the parameters leads to uncertainties in the model output variables, which are expressed as the 95% probability distributions. These are calculated at the 2.5% and 97.5% levels of the cumulative distribution of an output variable generated by the propagation of the parameter uncertainties using Latin hypercube sampling. This is referred to as the 95% prediction uncertainty, or 95PPU. These 95PPUs are the model outputs in a stochastic calibration approach. The model output represents an envelope of good solutions expressed by the 95PPU and generated by certain parameter ranges. It also shows the simulation that better adjusts to the observed values in accordance with the statistical value targeted (Abbaspour et al., 2007a, 2007b). Here, we only show the best calibration and simulation models as a continuous graph.

SWAT simulates evapotranspiration, infiltration, percolation, runoff generation, nutrient cycling and transport, biomass and crop yield for each HRU. Water flow as well as in-stream nutrient processes are simulated along the channel length for each subwatershed (Neitsch et al., 2005). A number of output files are generated in every SWAT simulation, i.e. the summary output file (output.std), the subwatershed output file (output.sub), and the main channel or reach output file (output.rch). The standard output summary file provides watershed average loadings from the HRUs to the streams on annual, monthly or daily basis. The subwatershed output file (output.sub) contains summary information for each of the subwatersheds in the watershed. The reported values for the different variables are the total amount or weighted average of all HRUs within the subwatershed. The variables include actual evapotranspiration

Table 1
Doses of water irrigation and fertilizers used as supplies for the major crops of the study area. (Dose units are kg ha^{-1}, except for swine manure which are m^3 ha^{-1}).

	Rice		Winter wheat		Winter barley		Corn		ALFALFA	
	Dose	Date	Dose	Date	Dose	Date	Dose	Date	Dose	Date
Basal fertilization	300 (urea)	April	700 (8-15-15)	November	600 (8-15-15)	November	1000 (8-15-15)	April		
Sowing time		April		November		November		April		April–September
Foliar fertilization			250 (urea)	February	200 (urea)	February	400 (urea)	May	350 (urea)	February
			150 (N liquid)	March	100 (N liquid)	March	200 (N liquid)	June	300 (urea)	June
Irrigation	11,000–13,000 m^3 ha^{-1}	May–September					8000–10,000 m^3 ha^{-1}	May–October	8000–10,000 m^3 ha^{-1}	Abril-October
Harvest		October		July		June		November		September (each 4 years)
Swine manure	30	Winter	30	Winter	30	Winter	60	Winter		

(ET); soil water content (SW), which is the amount of water (mm) in the soil profile; water yield (WYLD), which is the net amount of water (mm) that leaves the subwatershed and contributes to streamflow in the reach and water that percolates (PERC) past the root zone during the time step (mm); nitrate loading of groundwater (GWNO3), which is the amount of nitrate discharging below 100 cm of the root zone of the soil from the subwatershed (kg N ha^{-1}); and NO_3^- in lateral flow (NO3LATQ) per day in the subwatershed (kg N ha^{-1}). There is no groundwater NO_3^- measurement for calibration and all data related to the aquifer are estimated by the model. The main channel output file (output.rch) contains summary information for each routing reach in the watershed, including the average daily stream flow out (FLOW_OUT) of the reach during the time step (m^3 s^{-1}) and nitrate transported (NO3_OUT) with water out of the reach (kg N). The watershed model was calibrated and validated at the river outlet for all sub catchments together.

All these data calibrated and validated with SWAT-CUP, were used to quantify the spatial and temporal variations of green water storage (soil water content), green water flow (evapotranspiration), blue water (water yield plus deep aquifer recharge) and nitrate transport and infiltration at the Flumen watershed scale.

4. Results

4.1. Modeling water and nitrate discharges in Flumen River

A significant relationship between monthly water discharge data modeled and those recorded in situ was observed for both the calibration (NS = 0.62 and R^2 = 0.63) and the validation periods (NS = 0.51; R^2 = 0.52) (Table 2). Additionally, a high relationship was observed between both series of data at the daily scale (NS = 0.41 and R^2 = 0.42) for the calibration period and (NS = 0.52 and R^2 = 0.53) for the validation period.

An overestimation of the water discharges modeled with SWAT at the monthly scale was observed with respect to the data recorded in situ during the wintertime (November–March). In contrast, an underestimation was observed during the warm months (May–September) at the same monthly scale (Fig. 3A). Similar differences were observed between the two series of data at the daily scale (Fig. 3B), particularly at the peak discharges.

Rainfall showed seasonal cycles. It was higher in spring (May 2007, 2008 and 2009) and in autumn in 2008. Short rainfall events were also observed as river peak discharges at the watershed outlet. During the last few years, more frequent and intense rainfall events occurred with corresponding increased river flows in periods of time as short as hours or a few days (Darwiche-Criado et al., 2015a, 2015b). However, rainfall was only 45% of the inputs of water in the Flumen watershed. The remaining 55% was contributed through irrigation canals from two other rivers outside the Flumen watershed (Fig. 1D). The IRF resulted in lateral flow and contributed to the maintenance of a high base flow in the river throughout the year (Fig. 2). Rainfall regulated peak discharges, while the water exceeding irrigation contributed to maintain a minimum water discharge during most of the year.

With respect to nitrate, simulated and observed data maintained a strong relationship at the monthly scale for the calibration period (Table 3), with underestimation during some months (April, June, July 2010). Overestimation was observed during the validation period. Nitrate peak discharges in winter coincided with increased rainfall and periods of agricultural fertilization (Fig. 3C). The results of the simulation did not show a significant relationship with observed data on a daily basis. The variety of crops, the amount of fertilizer, the number of applications through the year and the application of pig slurry as fertilizer increased the uncertainty of the scheduled management operations for daily calibration. Monthly calibration does not need such precise temporal information. A delay was observed between the dates of application of basal fertilizer (Table 1) and the increase of nitrates in the river during winter. This did not occur during the period of foliar fertilization, as the detection of nitrate in the river is immediate. This was due to the composition of the fertilizer, since the basal fertilizer has to stay longer in the soil, so it can be used during the germination phase and the first moments of plant growth, and thus its mobility is reduced. Foliar

Table 2
Summary of the statistics results of modeling water and nitrate discharges in Flumen River.

Model evaluation techniques	Flow				Nitrate	
	Monthly		Daily		Monthly	
	Calibration	Validation	Calibration	Validation	Calibration	Validation
Number data point used	36	12	1461	730	8	8
p_factor	1	1	0.98	0.99	1	1
r_factor	0.33	0.72	0.78	0.22	0.75	1.02
R^2	0.63	0.52	0.42	0.53	0.64	0.72
NS	0.62	0.51	0.41	0.52	0.64	0.63
RSR	0.62	0.7	0.77	0.69	0.6	0.61
PBIAS	1.5	2.1	−2.2	−3.2	0.4	−2.4

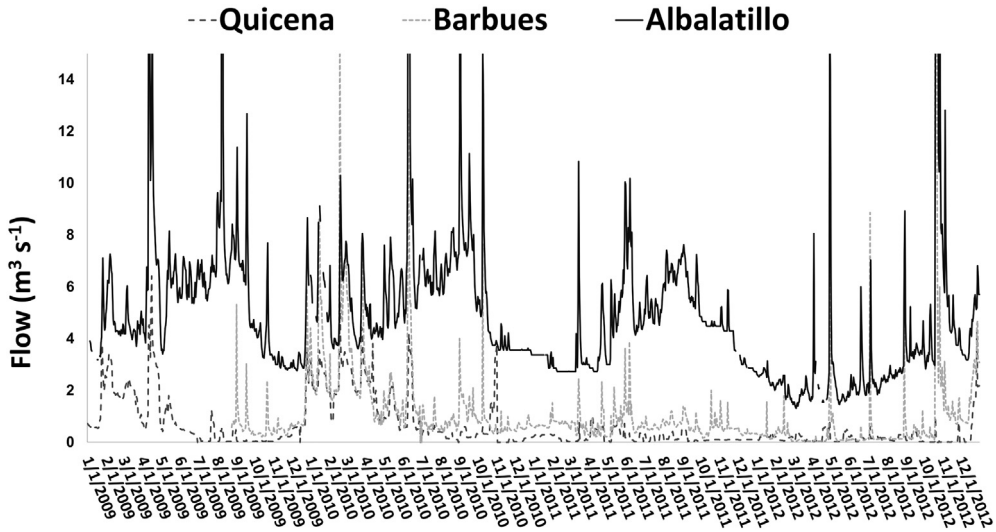

Fig. 2. Water discharge as recorded at three gauging stations in Flumen River: Quicena is located in the non-irrigated part of the watershed; Barbues and Albalatillo at the beginning and the end, respectively, of the irrigated area of the watershed.

fertilizer must be prepared to be readily absorbed by the plants, which are highly functional during the period of application of this type of fertilizer. Therefore, it is quickly absorbed by the plants, but it is also highly mobilized by irrigation water.

The results of the sensitivity analysis performed with SWAT-CUP showed that the parameters selected to estimate water discharge in Flumen River were sensitive. That is, small variations of these parameters negatively affected the calibration (Table 3).

The parameter with the highest sensitivity for water flow was the effective hydraulic conductivity in the main river alluvial channel (t-Stat CH_K2 = 2.47). The Flumen river increases its flow downstream by recharge with surface water and groundwater. The parameter CH_K2 is an indicator of the relationship between the riverbed and the aquifer. Low values of CH_K2 (0–500 mm h^{-1} is the SWAT range), as is our case (Table 3), indicate that there was hardly any contribution of water from the river to the aquifer, and therefore, the water balance of the watershed is positive in the flow of the river and increases as it approaches to its mouth.

Another sensitive parameter is the aquifer recharge delay (t-Stat GW_DELAY = 2.25), which represents the delay in days of water since the water passes from the ground to the aquifer and depends on the depth at which the aquifer is located and the hydraulic properties of the soil. In our case, the water percolates slowly until it reaches the aquifer (approximately 200 days according to the modeling results). This information is complementary to the previous parameter, since it shows the scarce and slow recharge of the aquifer from the channels or from the soil surface.

With respect to nitrates, the water content threshold that marks the limit for denitrification (t-Stat SDNCO = 18.18) and the organic matter mineralization rate (t-Stat CMN = 1.30) were the most sensitive parameters in the calibration process. This indicates the strong relationship between the biogeochemical processes represented by these two parameters and the nitrate concentration in the river.

The study area is drained by a dense network of excavated channels that determines the major water flow towards the Flumen River. Water flow from the superficial aquifer and lateral flow are the most relevant water flows through the soil at 36% and 43% of the total water circulating through the soil, respectively. The rest is surface flow and percolation towards the deep aquifer.

4.2. Water resources and quality in Flumen River watershed

In quantitative terms, green water storage (soil moisture) and, subsequently, green water flow (evapotranspiration) were the dominant components of the water balance in the Flumen River watershed. This makes sense because there is such an important contribution of water for irrigation, which mostly goes to green water and part of it to green water flow (Fig. 4).

The subwatersheds with the most blue water (20–40 mm $year^{-1}$ of water yield plus deep aquifer recharge) were located in the central irrigated zone (Fig. 5A. subwatersheds 5, 8, 9, 12, 13 and 18), highlighting a small subwatershed (number 4) where the tributary Isuela River meets the Flumen River (50–55 mm $year^{-1}$). In these subwatersheds, there was a supply of irrigation water for two-thirds of the year, which increased the amount of blue water. The subwatersheds with less blue water (5–20 mm $year^{-1}$) were located in the non-irrigated zone, with dry cereals and forest as major land uses (subwatersheds 1, 2, 3, 4, 6, 10, 14 and 19). The subwatersheds with higher blue water showed a similar temporal variability, with coefficients of variation (CV) between 60 and 90% (Fig. 5G). In contrast, the subwatesheds with low blue water differed in their CV (Fig. 5B). High temporal variability (70–110%) was observed in those in the north (subwatersheds 1, 2 and 3) and south (subwatersheds 14, 16 and 19) while those in the non-irrigated zones of the central part of the watershed showed the lowest temporal variability, <40% (subwatersheds 4 and 10).

Green water storage was quite similar (10–30% coefficients of variation) and low (50–70 mm $year^{-1}$) in the subwatersheds dominated by irrigation agriculture (subbasins 5, 8, 11, 12 and 13). On the contrary three small subwatersheds in the center and at the outlet of the Flumen watershed (subwatersheds 7, 9 and 18) had a high green water content (>100 mm $year^{-1}$) (Fig. 5C). The rest of subwatersheds, mostly located in the non-irrigated zone of the Flumen watershed, showed quite different green water contents, with CV ranging between 30 and 80% (Fig. 5D. subwatersheds 1, 2, 3, 4, 6, 10, 14 and 19).

The green water flow (Fig. 5E) represents the actual evapotranspiration. The highest values corresponded to the subwatersheds with irrigated agriculture (subwatersheds 5, 7, 8, 9, 11, 12, 13, 15, 16, and 18) as a major land use (40–60 mm $year^{-1}$). The rest of the subwatersheds in the north and south zones of the study area (subwatersheds 1, 2, 3, 6, 10, 14 and 19), which are occupied by large areas of dry agriculture, had low green water flows (20–40 mm $year^{-1}$). The temporal variability of green water flow (Fig. 5F) was higher in the upper part of the watersheds and tended to decrease towards the south (values approximately 70% in the north and 55% in the south).

In the subwatersheds with higher water availability from precipitation (subwatersheds 1 and 3) or irrigation (subwatersheds 7, 8, 9, 13, 15

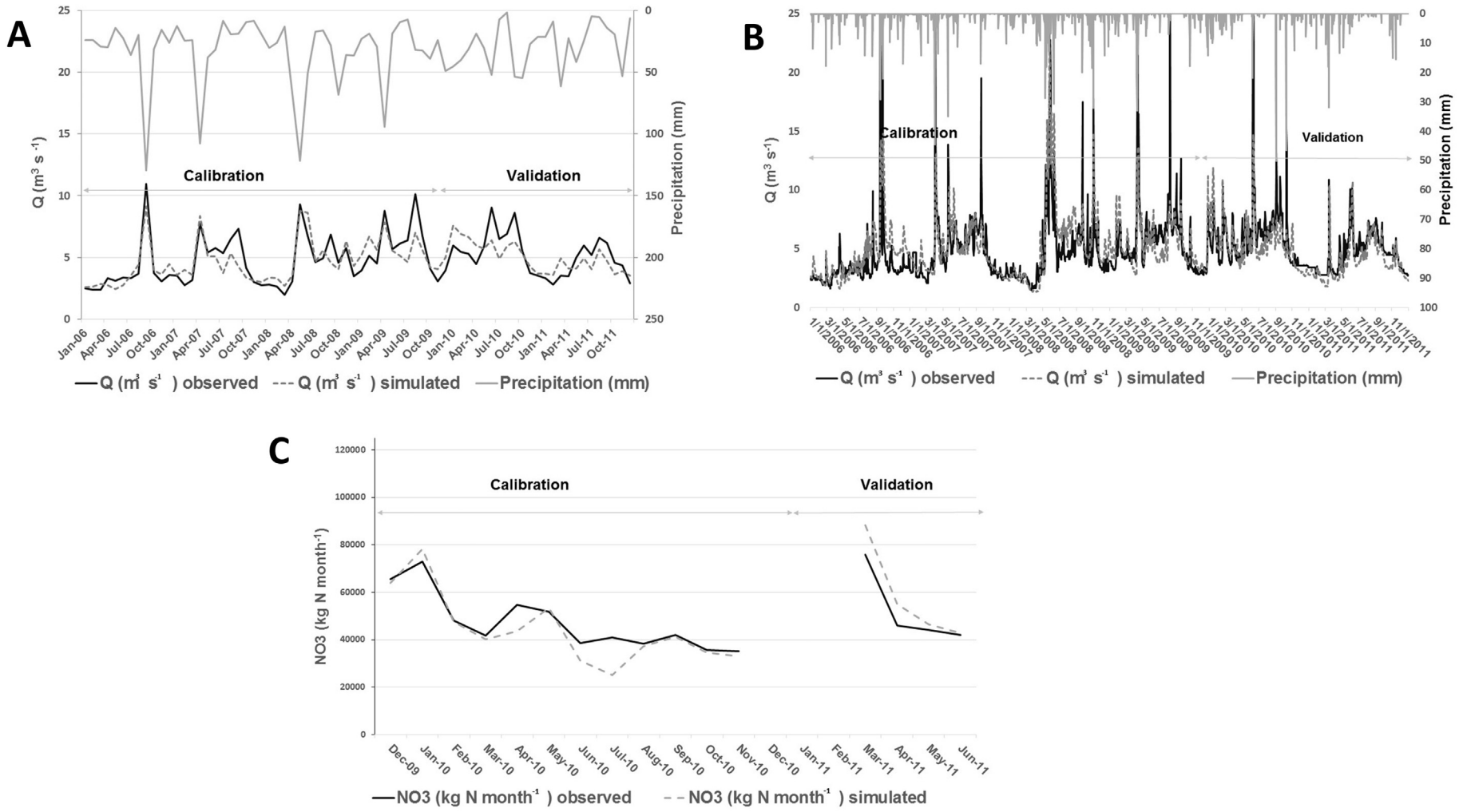

Fig. 3. A. Monthly water flow observed and simulated at the outlet, Albalatillo station, of River Flumen. Calibration period 2006–2010; validation period 2010–2011. Rainfall is represented as monthly average precipitation of the five weather stations. B. Daily water flow observed and simulated at the outlet, Albalatillo station, of the Flumen river. Calibration period 2006–2010; validation period 2010–2011. Rainfall is represented as daily average precipitation of the five weather stations. C. Nitrate observed and simulated in Flumen River at the outlet of River Flumen at monthly scale. Calibration period December 2009–December 2010; validation period January 2011–July 2011.

Table 3
SWAT Sensitivity analysis and calibration results in Flumen river watershed.

	Parameter Name	Definition	t-Stat	P-Value	Min value	Max value
Parameter sensitive to water discharge	V__CH_K2.rte	Effective hydraulic conductivity in main channel alluvium (mm hr^{-1})	2.47	0.01	5.59	9.48
	V__GW_DELAY.gw	Groundwater delay time (days)	2.25	0.02	138.17	283.48
	V__RCHRG_DP.gw	Deep aquifer percolation fraction	−1.94	0.05	0.12	0.36
	V__SLSUBBSN.hru	Average slope length (m)	1.21	0.23	123.37	139.64
	V__REVAPMN.gw	Threshold depth of water in the shallow aquifer for "revap" or percolation to the deep aquifer to occur (mm H2O)	1.13	0.26	169.98	240.22
	R__SOL_AWC(..).sol	Available water capacity of the soil layer (mm H2O mm $soil^{-1}$)	−1.11	0.27	−0.01	0.08
	V__SURLAG.bsn	Surface runoff lag coefficient	−1.05	0.3	7.89	9.2
	V__GW_REVAP.gw	Groundwater from the shallow aquifer into the overlying unsaturated zone coefficient	1	0.32	0.06	0.09
	R__SOL_K(..).sol	Saturated hydraulic conductivity (mm hr^{-1})	0.96	0.34	0.03	0.13
	V__OV_N.hru	Manning's "n" value for overland flow	−0.85	0.4	10.38	15.03
	V__ALPHA_BF.gw	Baseflow alpha factor (1 $days^{-1}$)	−0.81	0.42	0.24	0.37
	R__SOL_BD(..).sol	Soil bulk density (g cm^{-3})	0.78	0.43	−0.08	0.05
	V__ESCO.bsn	Soil evaporation compensation factor	0.58	0.56	0.32	0.46
	V__GWQMN.gw	Threshold depth of water in the shallow aquifer required for return flow to occur (mm H2O)	0.44	0.66	604.13	1155.01
	R__CN2.mgt	Initial SCS runoff curve number for moisture condition II	0.41	0.68	−0.06	0
	R__SOL_Z(..).sol	Depth from soil surface to bottom of layer (mm)	−0.2	0.84	−0.25	−0.1
Parameter sensitive to nitrate	V__SDNCO.bsn	Denitrification threshold water content	18.18	0	1.03	1.13
	V__CMN.bsn	Rate factor for humus mineralization of active organic nutrients	1.3	0.19	0.003	0.003
	V__HLIFE_NGW.gw	Half-life of nitrate in the shallow aquifer (days)	1.22	0.22	112.56	156.17
	V__NPERCO.bsn	Nitrate percolation coefficient	1.21	0.23	0.384	0.384
	V__N_UPDIS.bsn	Nitrogen uptake distribution parameter	−0.89	0.37	33.94	64.21
	V__SOL_NO3(..).chm	Initial NO3 concentration in the soil layer (mg kg of $soil^{-1}$)	0.77	0.44	54.61	63.07
	V__FRT_SURFACE{..}.mgt	Fraction of fertilizer applied to top 10 mm of soil	0.61	0.54	0.28	0.34
	V__CDN.bsn	Denitrification exponential rate coefficient	0.18	0.86	1.21	1.64

and 18), it is quickly transformed into green water flow because the climate of the study area is semi-arid with high temperatures. Therefore, it is in these subwatersheds where the greatest CV was observed (Fig. 5I).

Nitrate infiltration (Fig. 6A) in the aquifer was higher in the inner irrigated subwatersheds, with 100–250 kg N ha^{-1} $year^{-1}$ (subwatersheds 5, 8, 11, 12 and 13). However, these rates were not significant compared with lateral flow rates (Fig. 6B). The highest lateral nitrate flows were observed in the S-SW (subwatersheds 6, 10, 14 and 19), with 1400–2000 kg N ha^{-1} $year^{-1}$. These are the zones in the Flumen watershed with the highest slope and where nitrate consumption by biomass (dry cereals, scrubland and Mediterranean woods) was the lowest. As a result, nitrate lateral flow was directly related to average slope of the subwatersheds (Figs. 1C and 7 A), except in subwatershed 1. In the irrigated area (subbasins 5, 7, 8, 9, 11, 12, 13, 16, and 18), the lateral nitrate flow varied between 600 and 1400 kg N ha^{-1} $year^{-1}$, while in subwatershed 1, located in the north, and 7, in the center of the study area, it was lower than 400 kg N ha^{-1} $year^{-1}$ (Fig. 6B).

Additionally, a direct relationship was observed between nitrate infiltration and blue water, except for subwatershed 7, which is next to a river section where blue water, green water

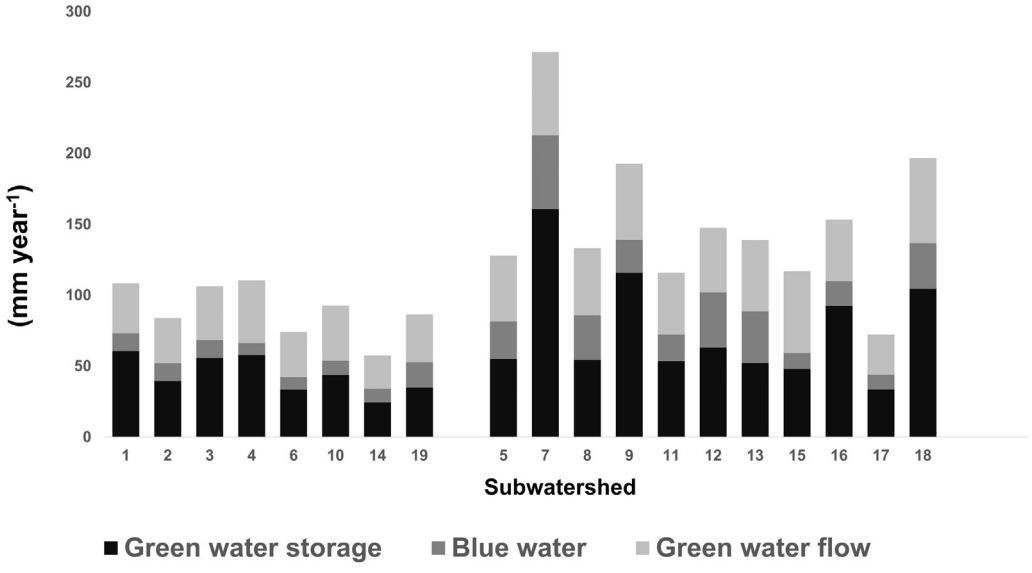

Fig. 4. Simulation of the average water balance for each subwatershed of the River Flumen watershed.

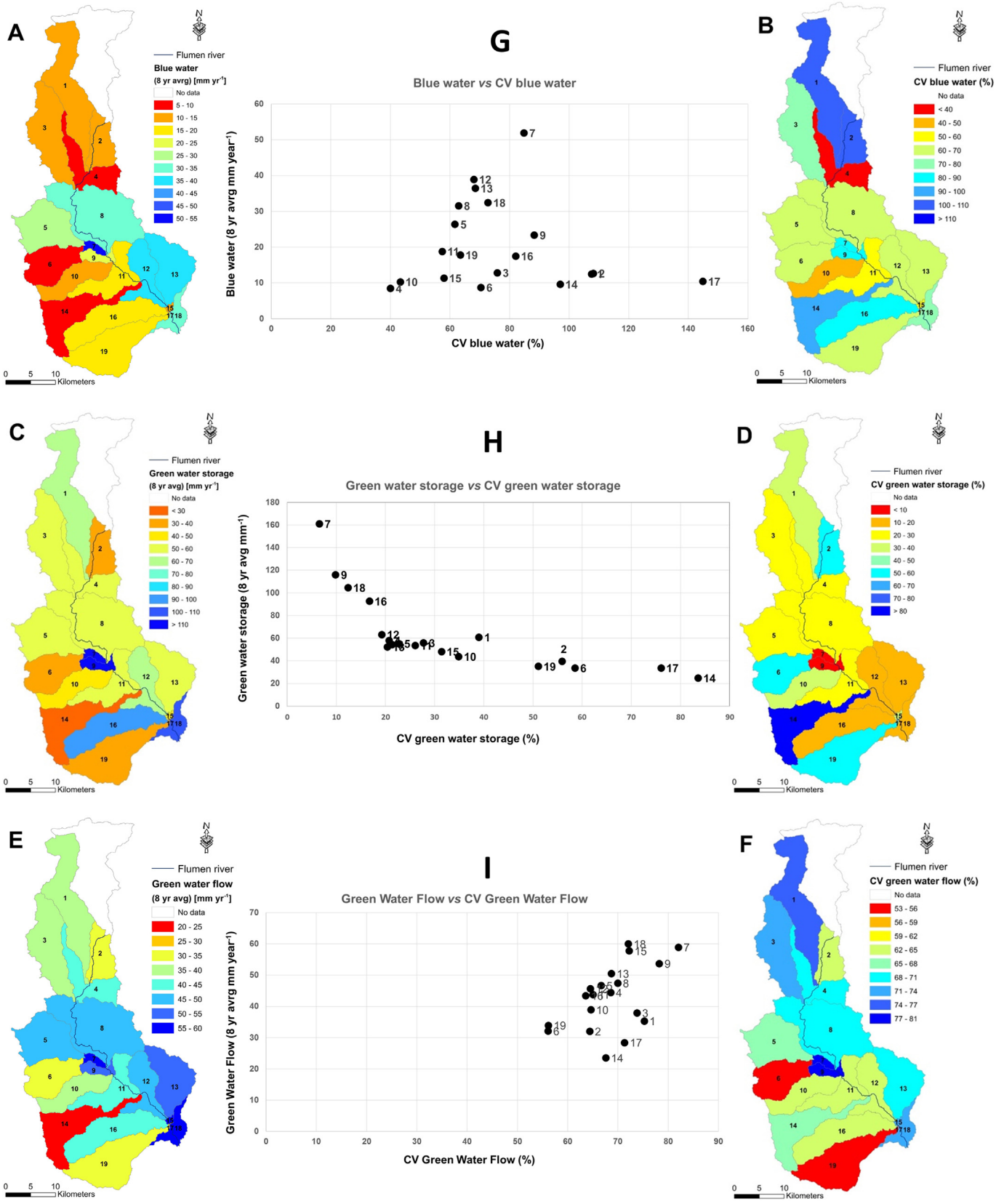

Fig. 5. Annual rates of blue water and green water in the different subwatersheds of River Flumen Watershed estimated after the SWAT model: A. blue water; B. Monthly coefficient of variation (CV) of blue water; C. Green water storage; D. Monthly CV of green water storage; E. Green water flow (evapotranspiration), and F. Monthly CV of green water flow. G. Blue water versus CV of blue water. H. Green water storage versus CV green water storage. I. Green water flow versus CV green water flow.

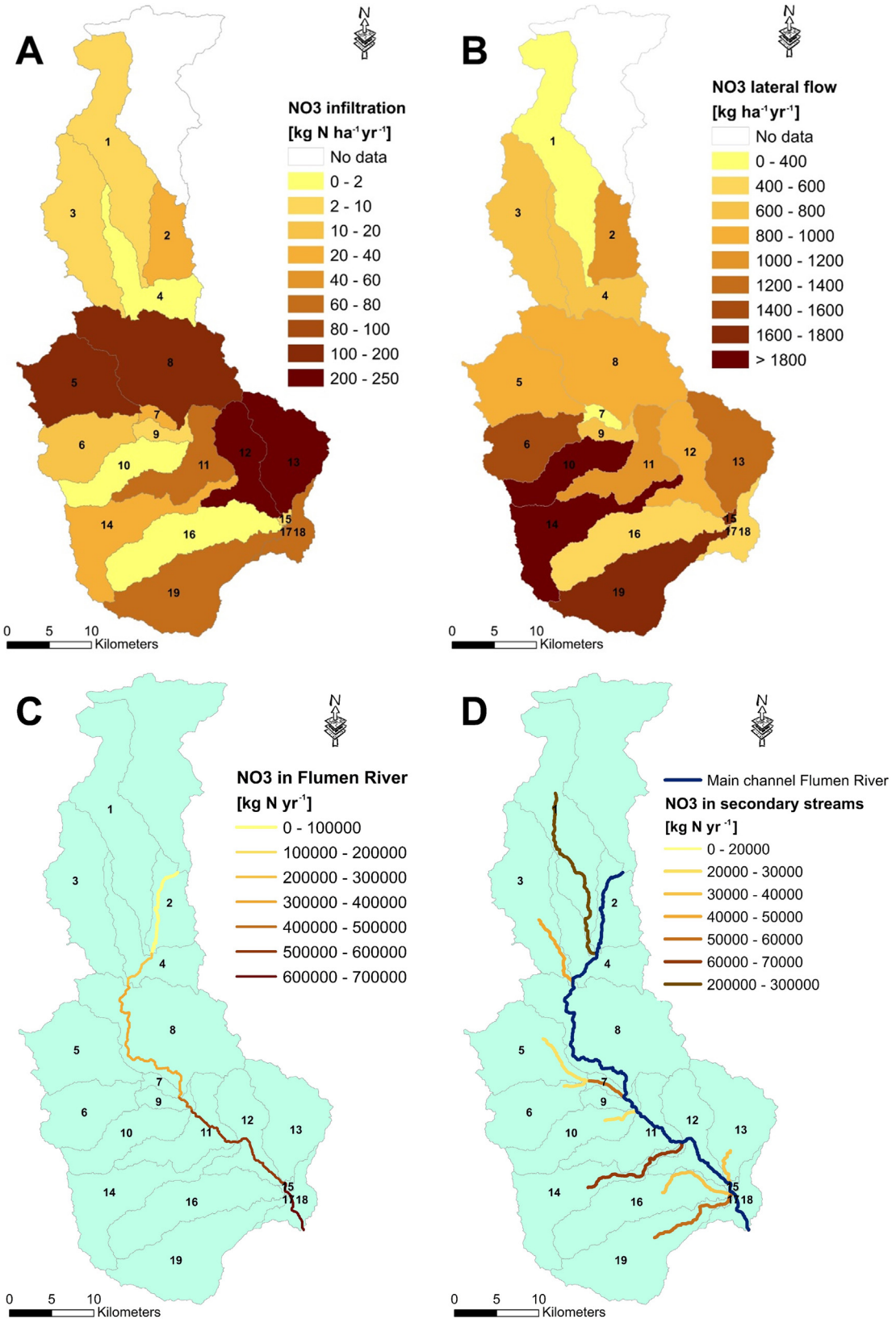

Fig. 6. A. Nitrate infiltration; B. Nitrate transported in lateral flow; C. Nitrate transported in the Flumen River; D. Nitrate transported in secondary streams discharging to Flumen River.

storage and flow were high and water infiltration was low (Fig. 7B). However, in contrast to what it could be expected, there was no clear relationship between nitrate infiltration and lateral flow (Fig. 7C).

A high amount of nitrate was exported annually throughout the Flumen watershed (700 tons N year^{-1}), as estimated with SWAT archive output.rch using average water flows (Fig. 6C). However, the average nitrate concentration in the Flumen River did not exceed

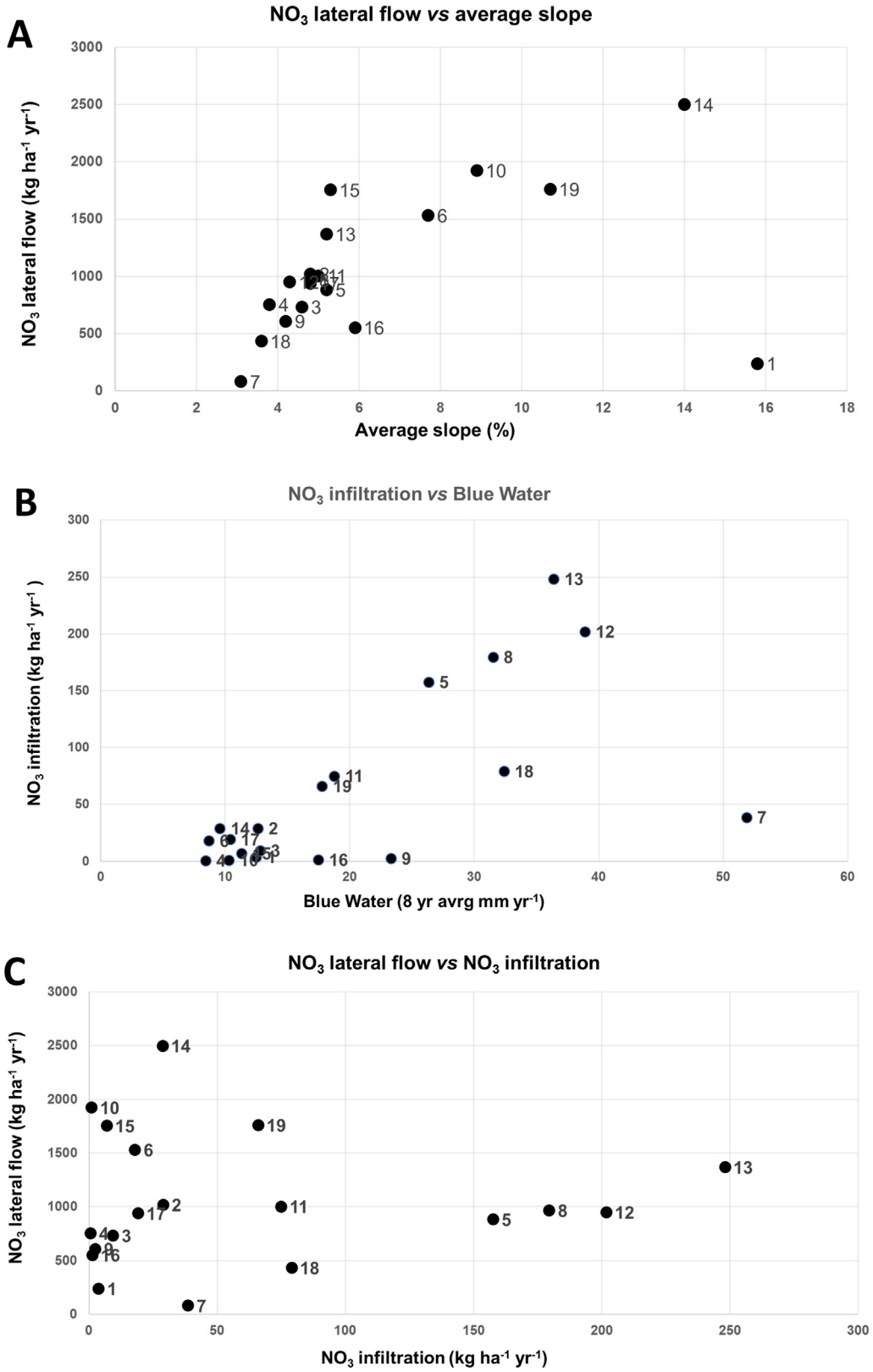
A
NO3 lateral flow vs average slope
NO3 lateral flow (kg ha-1 yr-1)
Average slope (%)
B
NO3 infiltration vs Blue Water
NO3 infiltration (kg ha-1 yr-1)
Blue Water (8 yr avrg mm yr-1)
C
NO3 lateral flow vs NO3 infiltration
NO3 lateral flow (kg ha-1 yr-1)
NO3 infiltration (kg ha-1 yr-1)

Fig. 7. A. Relationship between lateral nitrate flow and average slope of each subwatershed; B. Relationship between nitrate infiltration and blue and C. Relationship between lateral nitrate flow and nitrate infiltration in the Flumen River Watershed.

50 mg l^{-1}, except on October 10th, 2010. The largest subwatersheds discharged the highest amounts of nitrate to the Flumen River. This is the case for subwatersheds 14 and 19 in the SW part of the Flumen watershed, 50–70 tons N $year^{-1}$ (Fig. 6D). However, the highest amount was that of the Isuela River (subwatershed 1), in the north of the Flumen watershed, which contributed 200–300 tons N $year^{-1}$ of nitrates. This could be related to the fact that this tributary receives the discharge from the wastewater treatment plant of the city of Huesca.

5. Discussion

5.1. Modeling water and nitrate discharges in the Flumen River

A high statistical adjustment was obtained between modeled and observed values on a monthly basis for water (0.62 and 0.63 for NS and R^2, respectively) and nitrate (0.64 for both NS and R^2) discharges in the Flumen River despite the great complexity of the Flumen watershed, characterized by a very dense network of irrigation and drainage channels that drive the water flows. These results are similar to those obtained by other authors using SWAT to model water and nitrate (Table 4). According to Green et al. (2006) successful values for water and nitrate discharges in this type of studies are, respectively, >0.5 and >0.36 for NS and >0.7 and >0.5 for R^2, at this temporal scale.

The quality of the adjustment is related to the DEM resolution, since runoff of nitrogen is estimated from MUSLE (Williams and Berndt, 1977). Additionally, the scale of the soil map was confirmed as being of crucial importance for SWAT predictions of water runoff and nitrogen load estimations (Chaplot, 2005). The above-mentioned complexity of the Flumen watershed can be observed in Fig. 1, where land use types, irrigation and drainage networks and pig farms are represented. There are 1500 pig farms with a total population of 600,000 pigs located all around the Flumen basin. The pig slurry from these farms is used as fertilizer for the agricultural fields and is the origin of 55% of the nitrogen input (Lassaletta et al., 2012). All these characteristics add uncertainty to the model and affect its calibration and validation, resulting in a great number of data not to be fitted within the 95PPU range at the daily scale. Most of this uncertainty came from the inaccuracy in estimating the amount of slurry applied with high spatial and temporal resolution and the absence of valid and real information from farmers.

Other authors working with SWAT obtained disparate results (Table 4). Chaplot et al. (2005) modeled monthly nitrate discharges in the Walnut Creek (Iowa, USA) watershed (51.3 km^2), with a R^2 of 0.56 and NS of <0.1. The model by Santhi et al. (2002) in the Bosque River (Texas, USA) watershed (4277 km^2) obtained higher values of the adjustment indexes ($R^2 = 0.72$ and NS = 0.57). Pohlert et al. (2005) obtained significant results at the monthly scale in the Dill River watershed (Germany) (NS = 0.57 and 0.42 for the calibration and validation periods, respectively). In contrast, Lenhart et al. (2002), also working with data from the Dill River watershed, obtained much lower values of NS for nitrate discharge at the daily scale (0.31 and 0.09 for the periods of calibration and validation, respectively). Grizzetti et al. (2003) also obtained a low adjustment (NS = 0.30) when modeling non-point discharges and the retention of nutrients at the monthly scale with data from the Wantaanjoki watershed (Finland).

In our case, the major interest of daily modeling was to simulate the monthly data peaks that do not offer a good adjustment. In Mediterranean zones, some events (from minutes to a few hours) can accumulate a high part of the annual water and nitrate discharges (Darwiche-Criado et al., 2015a, 2015b). Our daily simulations in the Flumen watershed reflect sudden events of water discharges although these were underestimated by 10–30%. In some cases, these peaks were not estimated (September 2007, 2008, 2009, 2010). Then, our modeled daily water discharge was an underestimation of the observed data. Parameters such as CN2, CH_K or ALPHA_BF (Table 3) regulate the water discharge peaks. The best calibration results were obtained after the adjustment of the base water discharge rather than after the adjustment of water discharge peaks.5.2 Water resources and quality in the Flumen River watershed.

The water supplied for irrigation in the Flumen River watershed marks the seasonality of the water cycle (highly modifying the storage and flow of blue and green water) and reduces its annual CV (Fig. 5B and D). Then, land use is the main factor explaining the differences of blue and green water between subwatersheds.

On the other hand, the availability of irrigation water during summer determined that the flow of green water is high in quantity and with important temporal variation. In the zones of the study area where no irrigation is present, the typical seasonality of Mediterranean areas occurs, as seen in the rainfall regime (Fig. 3B and C). High amounts of water exceeding irrigation diluted the nitrogen exported from the agricultural zone, keeping nitrate concentrations in the river relatively low.

Our SWAT model showed an increasing discharge of nitrate as water flows along the Flumen River (Fig. 6C), which is related to the increasing irrigated area discharging irrigation return flows to the river. This is in agreement with in situ data collected by other authors relating the water characteristics of the river with land uses in different parts of the watershed (Darwiche-Criado et al., 2015a, 2015b). We estimated a nitrate discharge of up to 600,000 kg N $year^{-1}$ at the river mouth (Fig. 6C). We also showed that the highest nitrate discharges in subwatersheds were those in the central-south part of the watershed, which showed a higher lateral flow of water (Fig. 6). This nitrate discharges were associated with nitrate lateral flows and coincide with the watersheds that have higher coefficients of variation of these nitrate lateral flows. Nitrate is accumulated in the soil, and a large part of it is mobilized in large quantities in short periods of time (a few hours to a few days) and discharged to the river, coinciding with periods of intense rainfall, shown as hysteresis cycles of the nitrate concentration in River Flumen. However a general positive correlation between nitrate and water discharge in the river is observed both for the irrigation and the non-irrigation periods of the year (Darwiche-Criado et al., 2015a, 2015b).

The highest values of nitrate infiltration were observed in the irrigated agricultural zone (Fig. 6A). Lateral nitrate flows were not directly

Table 4
NS and R^2 results of similar SWAT modeling studies. Land use refers the percentages of major land use types in the respective study areas.

	Author					
	Chaplot et al. (2004)	Santhi et al. (2002)	Pohlert et al. (2005)	Lenhart et al. (2003)	Grizzeti et al. (2003)	Present study
Flow						
Landuse						
Pasture		15	21	21		18
Forest/range		64	55	57	60	14
Crops	90	17	7	6	30	66
Calibration						
Daily						
R2						0.42
NS			0.81		0.66	0.41
Monthly						
R2	0.73	0.89				0.63
NS	0.27	0.83			0.76	0.62
Validation						
Daily						
R2			0.6			0.53
NS		0.92	0.56			0.52
Monthly						
R2		0.87				0.52
NS						0.51
Nitrate						
Calibration						
Daily						
R2				0.78		
NS			0.15	0.26	0.51	
Monthly						
R2	0.56	0.72	0.69			0.64
NS	0.005	0.57	0.66		0.3	0.64
Validation						
Daily						
R2				0.58		
NS				0.09		
Monthly						
R2		0.72	0.77			0.72
NS		0.43	0.7			0.63

related to nitrate infiltration in the soil (Fig. 7C), suggesting that the soil has a high capacity to accumulate nitrate, and its release from the soil-aquifer system towards the river is regulated by the internal, hydraulic conductivity characteristics of the soil, slope and external factors, such as rainfall events, that cause high water infiltration in the soil and lateral discharges. Causapé et al. (2004) studied a small watershed close to our study area with similar characteristics close to our study area. Their soil water balance also showed that irrigation was a key factor for the seasonal water quality and quantity due to return flows from irrigation, with flow peaks resulting from surface runoff and fast drainage of fields, as well as direct spillover of irrigation water into drainage ditches.

Flat topography also favors the vertical infiltration of water and nitrate towards the aquifer in the flat irrigated zone of the Flumen watershed. In contrast, the subsurface lateral flow of nitrate was higher in subwatersheds with higher slopes (subwatersheds 6, 10, 14 and 19 (Fig. 6B), located in the outer zones of the Flumen watershed, which are occupied by dry cereals, shrub and woodlands (Fig. 1E). If natural vegetation, such as shrubs and pines, cover the land, there is an accumulation of plant biomass and nutrients, which are leached during rainfall events. These subwatersheds with higher lateral flow are zones where the incorporation of good agrarian practices, such as the reduction of chemical fertilization and timing irrigation and fertilizer applications in tight accordance with plant growth, could contribute to a more efficient use of fertilizers and decrease nitrate discharges to the Flumen River. These practices could be associated with promoting the use of plant varieties that require lower fertilization, if the commercial aspects are covered. Additionally, restoring river and field strip buffers and wetlands in secondary streams will also decrease the nitrate discharge to rivers in intensively irrigated agricultural territories (Borin et al., 2010; Mander et al., 2017).

In a semi-arid region, such as the Flumen River Basin, where the local economy is based mainly on irrigated agriculture, knowledge of water flows and the water balance is fundamental for the maintenance and improvement of the sector. In this type of area, prolonged periods of drought are frequent, which affects the availability of water for irrigation. Studies like this show how irrigation water is used by the plant cover and is transformed into green water flow (Fig. 5E) or how excess irrigation water increases blue water (Fig. 5G). In both cases, the blue water and green water flow are greater in the irrigated subwatersheds (Figs. 5A and E). The water used for irrigation in Flumen River watershed proceeds from reservoirs in rivers outside it. The water returned due to excess irrigation (IRF) generates flows in the hydrological network in the basin above those that would correspond to it due to climatic conditions (Fig. 2). Excess irrigation water contributes to the leaching of nitrates towards the aquifer, the drainage channels and rivers, altering the water quality (Figs. 6A and C).

In order to know the potential impacts of practical management actions on the water and nitrate discharges two scenarios were simulated with SWAT by combining a 10% increased temperature and 20% reduced precipitation which are foreseen climate change factors (Vicente-Serrano et al., 2015). In the first scenario 50% of the area used to cultivate the most demanding irrigated crops (rice, maize and alfalfa) is changed to irrigated cereal. This is an interesting scenario as water available for irrigation is frequently (once every five years) restricted in the study area because of reduced rainfall in the mountains providing the water for irrigation. In the second scenario a 40% reduction of the areal dose of nitrogen fertilization is applied. Both scenarios have been calculated for the period 2020 to 2040 (Supplementary material Scenarios) and have been taken into account the last three years of this scenario to obtain the percentages of change of water and nitrates flow.

After the first scenario, the water flow of River Flumen at the outlet of the watershed is reduced by 15%, especially in summer, when the cereal is not irrigated. The amount of nitrate exported is reduced by 10% and the sequence throughout the year is similar to the calibration period. The second scenario showed a small decrease in the river water flow (1–2%) and a marked reduction of nitrate discharge (28%). This decrease is particularly significant in winter months because of the smaller accumulation of excess fertilization in the soil than under the current situation. These results show a high potential to improve river water quality in intensively irrigated and fertilized territories, both managing land uses and fertilization dosing.

6. Conclusions

According to the data obtained from the modeling of the Flumen River watershed there was a direct relationship between land uses and water flows which carry nitrates to the aquifer and rivers, with greater infiltration in the irrigation zone and higher lateral flow of nitrates in the steep subwatersheds with rainfed agriculture. A high availability of blue water was observed in the irrigated agricultural area due to high irrigation doses. There is also a higher amount of green water flow due to the activity of the crops. On the other hand, the subwatersheds with dominance of rainfed cereals did not show a clear pattern regarding the availability of blue and green water. However, in these non-irrigated zones, the nitrate excess not taken up by the crops and that accumulated as biomass in the forest zones was moved out by intensive rain events towards the river. Although nitrates had not been calibrated on a daily scale there are a measured data in outlet gauging of flash floods and nitrate transport in these intensive rain events. This occured mainly in the subwatersheds with the highest slopes and where rainfall was more intermittent. We recommend to dose irrigation to decrease the use of blue water and the green water flow and, additionally, to dose the amount of fertilizer used, especially in dry cereal areas, where lateral nitrate flow is high, and timing their uses to the requirements of the crops. Future scenarios with reduction of irrigation and fertilizer inputs shows decrease in flow and transport of nitrates at the outlet of the watershed.

Acknowledgements

This work was supported by project AGUAFLASH (Interreg IVB SUDOE1/P2/F146) and AMUSE (CGL2014-53017 C2-1-R, Spanish Ministry of Economy and Competitiveness). Thanks are given to Nadia Darwiche-Criado and IPE-CSIC lab and field assistants. Also to “Comarca” and “Cooperativa Los Monegros” for their collaboration. CHE and SIRASA are acknowledged for providing basic data of the territory. This is a contribution of Aragon Research Group E40-17R.

Appendix A. Supplementary data

Supplementary data to this article can be found online at https://doi.org/10.1016/j.scitotenv.2018.12.023.

References

Abbaspour, K.C., Vejdani, M., Haghighat, S., Yang, J., 2007a. SWAT-CUP Calibration and Uncertainty Programs for SWAT. The Fourth International SWAT Conference. , pp. 1596–1602 https://doi.org/10.1007/s00402-009-1032-4.

Abbaspour, K.C., Yang, J., Maximov, I., Siber, R., Bogner, K., Mieleitner, J., ... Srinivasan, R., 2007b. Modelling hydrology and water quality in the pre-alpine/alpine Thur watershed using SWAT. J. Hydrol. 333 (2–4), 413–430. https://doi.org/10.1016/j.jhydrol.2006.09.014.

Arnold, J.G., Srinivasan, R., Muttiah, R.S., Williams, J.R., 1998. Large area hydrologic modeling and assesment part I: model development. J. Am. Water Resour. Assoc. 34 (1), 73–89. https://doi.org/10.1111/j.1752-1688.1998.tb05961.x.

Arnold, J.G., Moriasi, D.N., Gassman, P.W., Abbaspour, K.C., White, M.J., Srinivasan, R., Jha, M.K., 2012. Swat: Model Use, Calibration, and Validation. 55(4). Asabe, pp. 1491–1508. https://doi.org/10.13031/2013.42256 (ISSN 2151-0032).

Borin, M., Passoni, M., Thiene, M., Tempesta, T., 2010. Multiple functions of buffer strips in farming areas. Eur. J. Agron. 32 (1), 103–111. https://doi.org/10.1016/j.eja.2009.05.003.

Causapé, J., Quílez, D., Aragüés, R., 2004. Assessment of irrigation and environmental quality at the hydrological basin level: II. Salt and nitrate loads in irrigation return flows. Agric. Water Manag. 70 (3), 211–228. https://doi.org/10.1016/j.agwat.2004.06.006.

Causapé, J., Quílez, D., Aragüés, R., 2006. Irrigation efficiency and quality of irrigation return flows in the Ebro River basin: an overview. Environ. Monit. Assess. 117 (1–3), 451–461. https://doi.org/10.1007/s10661-006-0763-8.

Chaplot, V., 2005. Impact of DEM mesh size and soil map scale on SWAT runoff, sediment, and NO 3-N loads predictions. J. Hydrol. 312 (1–4), 207–222. https://doi.org/10.1016/j.jhydrol.2005.02.017.

Chaplot, V., Saleh, A., Jaynes, D.B., 2005. Effect of the accuracy of spatial rainfall information on the modeling of water, sediment, and NO3-N loads at the watershed level. J. Hydrol. 312 (1–4), 223–234. https://doi.org/10.1016/j.jhydrol.2005.02.019.

Comín, F.A., Williams, W.D., 1994. Parched continents: our common future? Limnology Now , pp. 473–527 Retrieved from. http://www.scopus.com/inward/record.url?eid=2-s2.0-0028576666&partnerID=40&md5=238b9a9ffd253d42b06f50f8e7a4c60f

Darwiche-Criado, N., Comín, F.A., Sorando, R., Sánchez-Pérez, J.M., 2015a. Seasonal variability of NO_3^- mobilization during flood events in a Mediterranean catchment: the influence of intensive agricultural irrigation. Agric. Ecosyst. Environ. 200, 208–218. https://doi.org/10.1016/j.agee.2014.11.002.

Darwiche-Criado, N., Jiménez, J.J., Comín, F.A., Sorando, R., Sánchez-Pérez, J.M., 2015b. Identifying spatial and seasonal patterns of river water quality in a semiarid irrigated agricultural Mediterranean basin. Environ. Sci. Pollut. Res. 22 (23), 18626–18636. https://doi.org/10.1007/s11356-015-5484-5.

Faramarzi, M., Abbaspour, K.C., Schulin, R., Yang, H., 2009. Modelling blue and green water resources availability in Iran. Hydrol. Process. 23 (3), 486–501. https://doi.org/10.1002/hyp.7160.

Ferrant, S., Laplanche, C., Durbe, G., Probst, A., Dugast, P., Durand, P., ... Probst, J.L., 2013. Continuous measurement of nitrate concentration in a highly event-responsive agricultural catchment in south-west of France: is the gain of information useful? Hydrol. Process. 27 (12), 1751–1763. https://doi.org/10.1002/hyp.9324.

Gassman, P.W., Sadeghi, A.M., Srinivasan, R., 2014. Applications of the SWAT model special section: overview and insights. J. Environ. Qual. 43 (1), 1–8.

Green, C.H., Tomer, M.D., di Luzio, M., Arnold, J.G., 2006. Hydrologic evaluation of the soil and water assessment tool for a large tile-drained watershed in Iowa. Trans. ASABE 49 (2), 413–422. https://doi.org/10.13031/2013.20415.

Grizzetti, B., Bouraoui, F., Granlund, K., Rekolainen, S., Bidoglio, G., 2003. Modelling diffuse emission and retention of nutrients in the Vantaanjoki watershed (Finland) using the SWAT model. Ecol. Model. 169 (1), 25–38. https://doi.org/10.1016/S0304-3800(03)00198-4.

Haddeland, I., Lettenmaier, D.P., Skaugen, T., 2006. Effects of irrigation on the water and energy balances of the Colorado and Mekong river basins. J. Hydrol. 324 (1–4), 210–223. https://doi.org/10.1016/j.jhydrol.2005.09.028.

Herrero, J., Hudnall, W.H., 2014. Measurement of soil salinity using electromagnetic induction in a paddy with a densic pan and shallow water table. Paddy Water Environ. 12, 263–274. https://doi.org/10.1007/s10333-013-0371-5.

Kaushal, S.S., Groffman, P.M., Mayer, P.M., Striz, E., Gold, A.J., 2008. Effects of stream restoration on denitrification in an urbanizing watershed. Ecol. Appl. 18 (3), 789–804. https://doi.org/10.1890/07-1159.1.

Lacroix, A., Laurent, F., Ruelland, D., Sauboua, E., 2006. Nitrate pollution risk assessment: from the model to the indicator. Int. J. Agric. Resour. Gov. Ecol. 5 (2), 206–223 Retrieved from. http://inderscience.metapress.com/index/AU5JMDBFN6WUG041.pdf.

Lassaletta, L., Romero, E., Billen, G., Garnier, J., García-Gómez, H., Rovira, J.V., 2012. Spatialized N budgets in a large agricultural Mediterranean watershed: high loading and low transfer. Biogeosciences 9 (1), 57–70. https://doi.org/10.5194/bg-9-57-2012.

Lenhart, T., Eckhardt, K., Fohrer, N., Frede, H.-G., 2002. Comparison of two different approaches of sensitivity analysis. Phys. Chem. Earth, Parts A/B/C 27 (9–10), 645–654. https://doi.org/10.1016/S1474-7065(02)00049-9.

Mander, Ü., Tournebize, J., Tonderski, K., Verhoeven, J.T.A., Mitsch, W.J., 2017, June 1. Planning and establishment principles for constructed wetlands and riparian buffer zones in agricultural catchments. Ecol. Eng. 103, 296–300. https://doi.org/10.1016/j.ecoleng.2016.12.006.

Moriasi, D.N., Arnold, J.G., Van Liew, M.W., Bingner, R.L., Harmel, R.D., Veith, T.L., 2007. Model evaluation guidelines for systematic quantification of accuracy in watershed simulations. Trans. ASABE 50 (3), 885–900. https://doi.org/10.13031/2013.23153.

Neitsch, S.L., Arnold, J.G., Kiniry, J.R., Srinivasan, R., Williams, J.R., 2005. Soil and Water Assessment Tool Input/Output File Documentation, Version 2005. Temple, Tex.: USDA-ARS Grassland. Soil and Water Research Laboratory. Available at:. http://swatmodel.tamu.edu/documentation 65(1–3), pp. 139–158. https://doi.org/10.1016/0022-1694(83)90214-7.

Oeurng, C., Sauvage, S., Sánchez-Pérez, J.M., 2011a. Assessment of hydrology, sediment and particulate organic carbon yield in a large agricultural catchment using the SWAT model. J. Hydrol. 401 (3–4), 145–153. https://doi.org/10.1016/j.jhydrol.2011.02.017.

Oeurng, C., Sauvage, S., Sánchez-Pérez, J.M., 2011b. Assessment of hydrology, sediment and particulate organic carbon yield in a large agricultural catchment using the SWAT model. J. Hydrol. 401 (3–4), 145–153. https://doi.org/10.1016/j.jhydrol.2011.02.017.

PNOA, 2009. Plan Nacional de Ortofotografía Aérea (PNOA) es un proyecto cofinanciado y cooperativo entre la Administración General del Estado (AGE) de España y las Comunidades Autónomas que se enmarca dentro del Plan Nacional de Observación del Territorio (PNOT), siendo coordinado por el Instituto Geográfico Nacional (IGN) y el Centro Nacional de Información Geográfica (CNIG).

Pohlert, T., Huisman, J., Breuer, L., Frede, H.G., 2005. Modelling of point and non-point source pollution of nitrate with SWAT in the river Dill, Germany. Adv. Geosci. 5, 7–12.

Rostamian, R., Jaleh, A., Afyuni, M., Mousavi, S.F., Heidarpour, M., Jalalian, A., Abbaspour, K.C., 2008. Application of a SWAT model for estimating runoff and sediment in two mountainous basins in central Iran. Hydrol. Sci. J. 53, 977–988. https://doi.org/10.1623/hysj.53.5.977.

Santhi, C., Arnold, J.G., Williams, J.R., Dugas, W.a., Srinivasan, R., Hauck, L.M., 2002. Validation of the SWAT model on a large river basin with point and nonpoint sources. J. Am. Water Resour. Assoc. 37 (5), 1169–1188. https://doi.org/10.1111/j.1752-1688.2001.tb03630.x.

Seitzinger, S.P., Harrison, J.A., 2008. Land-based nitrogen sources and their delivery to coastal systems. Nitrogen in the Marine Environment. Elsevier Inc., pp. 469–510 https://doi.org/10.1016/B978-0-12-372522-6.00009-8.

Srinivasan, R., Arnold, J.G., Jones, C.A., 1998. Hydrologic modelling of the United States with the soil and water assessment tool. Int. J. Water Resour. Dev. 14 (3), 315–325. https://doi.org/10.1080/07900629849231.

Tilman, D., Cassman, K.G., Matson, P.A., Naylor, R., Polasky, S., Chikowo, R., ... Li, L., 2002. Agriculture sustainability and intensive production practices. Nature 418 (August), 671–677. https://doi.org/10.1007/s13398-014-0173-7.2.

Ullrich, A., Volk, M., 2009. Application of the soil and water assessment tool (SWAT) to predict the impact of alternative management practices on water quality and quantity. Agric. Water Manag. 96 (8), 1207–1217. https://doi.org/10.1016/j.agwat.2009.03.010.

Vicente-Serrano, S.M., Cabello, D., Tomás-Burguera, M., Martín-Hernández, N., Beguería, S., Azorin-Molina, C., El Kenawy, A., 2015. Drought variability and land degradation in semiarid regions: assessment using remote sensing data and drought indices (1982–2011). Remote Sens. 7, 4391–4423.

Williams, J.R., Berndt, H.D., 1977. Sediment yield prediction based on watershed hydrology. Trans. Am. Soc. Agric. Eng. 20 (6), 1100–1104. https://doi.org/10.13031/2013.35710.